

# Accuracy of Divergence Measures for Detection of Abrupt Changes

P. Bergl

**Abstract**—Numerous divergence measures (spectral distance, cepstral distance, difference of the cepstral coefficients, Kullback-Leibler divergence, distance given by the General Likelihood Ratio, distance defined by the Recursive Bayesian Change-point Detector and the Mahalanobis measure) are compared in this study. The measures are used for detection of abrupt spectral changes in synthetic AR signals via the sliding window algorithm. Two experiments are performed; the first is focused on detection of single boundary while the second concentrates on detection of a couple of boundaries. Accuracy of detection is judged for each method; the measures are compared according to results of both experiments.

**Keywords**—Abrupt changes detection, autoregressive model, divergence measure.

## I. INTRODUCTION

A divergence measure can be used for detection of abrupt changes in signals. For many applications (speech recognition, EEG analysis), spectral changes are the most interesting. It is well known that a great number of real signals can be modeled as an autoregressive (AR) model. This approach is used in this study; synthetic AR signals with abrupt spectral changes are generated. Our task is to compare some chosen detectors according to the accuracy of detection. A similar topic has been described for many types of distance or divergence measure, e.g. [1]. This work is unique in its use of a large number of measures; each measure is used with a variety of adjustments.

## II. METHODS AND EXPERIMENTS

Let's assume a distance measure  $d(s_1, s_2)$ , where  $s_1$  and  $s_2$  is a signal; the value of  $d(s_1, s_2)$  is equal to spectral divergence of the signals. The simplest example of such a measure is difference of spectra  $d_{FFT} = \frac{1}{N} \sqrt{S_1 - S_2}$ , where  $N$  is length of the signal (the same length of the signals is assumed for simplicity),  $S_1$  and  $S_2$  is spectra calculated via the FFT (Fast Fourier Transformation).

A distance measure can be used for analyzing a signal via the sliding window algorithm. Initially a window of length  $L$  is positioned at the beginning of the signal, signal  $s_1$  is defined by the left half of the window, signal  $s_2$  is defined by the right half. The distance measure can be then calculated. In the next step of the algorithm, the sliding window is moved one sample forward. New signals  $s_1$  and  $s_2$  are established and the distance measure is calculated again. This step is repeated until the end of the signal is reached. Finally, a set of values of the distance measure is obtained, each value

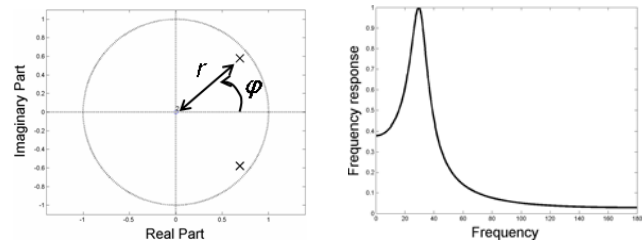


Fig. 1. Position of poles in complex  $z$ -plane and frequency response for  $r = 0.9$ ,  $\varphi = 30^\circ$ .

defines spectra difference in the left and right half of the sliding window with respect to the position of the window. These values can be plotted as a curve, where the time coordinate of the distance measure value is defined by the middle of the sliding window, meaning that the  $L/2$  first and  $L/2$  last samples of the curve are zero. The most important feature of the curve is that remarkable changes in spectra of the signal are indicated with local maxima of the curve. A demonstration of a synthetic autoregressive (AR) signal with abrupt spectral changes, its spectrogram and some calculated distance measures are displayed in Fig. 3.

The AR model is defined by the following

$$s(n) = - \sum_{i=1}^p b_i s(n-i) + G \cdot e(n), \quad n = p, \dots, N-1, \quad (1)$$

where  $p$  is the order of the model; coefficients  $b_i$  are called linear predictive coefficients (*lpc*);  $e(n)$  is white noise (i.e. with the Gaussian distribution, zero mean value and uncorrelated),  $G$  stands for gain. AR model assumes, that actual sample of the signal ( $s(n)$ ) is a linear combination of preceding  $p$  samples with additive noise  $e(n)$ . The AR model can be easily used for generating synthetic signals with defined spectral qualities. The definition (equation 1) is similar to formula of the IIR filtration; an AR signal can be generated using an IIR filter fed with white noise, with system function  $H(z)$  given by the parameters of the AR model:

$$H(z) = \frac{G}{1 + b_1 z^{-1} + \dots + b_p z^{-p}}. \quad (2)$$

The simplest case is for  $p = 2$ , then the system function is defined by a couple of complex poles. Position of the poles in complex  $z$ -plane is defined by two coordinates, radius  $r$ , and angle  $\varphi$  (see Fig. 1).

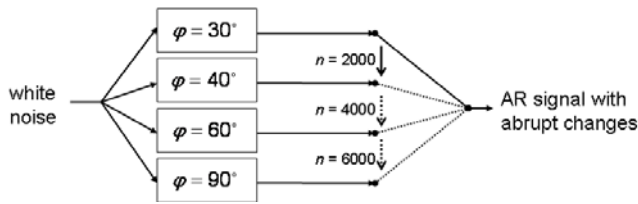


Fig. 2. Structure for generating of AR signal with three abrupt changes.

A. Experiment no.1: Abrupt Changes With Increasing Value of Spectral Divergence

A signal with abrupt spectral changes can be easily generated using various IIR filters with different position of the poles. A structure for generating the AR signal with three abrupt changes is shown in Fig. 2. It is made up of four IIR filters; all are fed with the same white noise. We subsequently switch from output of one filter to output of the next filter in defined time instants (for  $n = 2000, 4000, 6000$ ), the total length of the signal is 8000 samples; AR order 2 is assumed, parameters of the filters are following

- filter no. 1:  $r = 0.9, \varphi = 30^\circ$ ;
- filter no. 2:  $r = 0.9, \varphi = 40^\circ$ ;
- filter no. 3:  $r = 0.9, \varphi = 60^\circ$ ;
- filter no. 4:  $r = 0.9, \varphi = 90^\circ$ .

Difference between the angles is increasing (it is  $10^\circ$  for the first change,  $20^\circ$  for the second and  $30^\circ$  for the third). It implies that value of the spectral divergence is increasing as well, meaning the first change is "small", the second one is "medium" and the third one is "large". An example of the signal is displayed in Fig. 3.

A total number of 200 signals are generated, each one to be analyzed with numerous types of divergence measures, each measure is used with various settings ( $L$  stands for window length in samples):

- $d_{Bay}$  given by Recursive Bayesian Autoregressive Change-point Detector (RBACDN), see [3], [4];  $L \in \{600, 800, 1000\}$ ;
- $d_{GLR}$  given by General Likelihood Ratio, see [2];  $L \in \{400, 600, 800\}$ ;
- $d_{FFT}$ ;  $L \in \{600, 800, 1000\}$ ;
- $d_{Cep} = \frac{1}{N} \sqrt{c_1 - c_2}$ , where  $c_1, c_2$  stands for cepstrum of the signal;  $L \in \{600, 800, 1000\}$ ;
- $d_{CC}$ , given by difference of cepstral coefficients derived from coefficients of the AR model;  $L \in \{400, 600, 800\}$ ;
- $d_{Kull}$  given by the Kullback-Leibler divergence, see [6];  $L \in \{400, 600, 800\}$ ;
- $d_{Mah}$  defined by the Mahalanobis measure, see [5];  $L \in \{400, 600, 800\}$ ;

Note: The order of the AR model equals 2 for all methods which use the AR model.

Altogether 30 curves are obtained for each signal from the training set. The positions of three local maxima are detected in each curve. These maxima represent the estimated positions

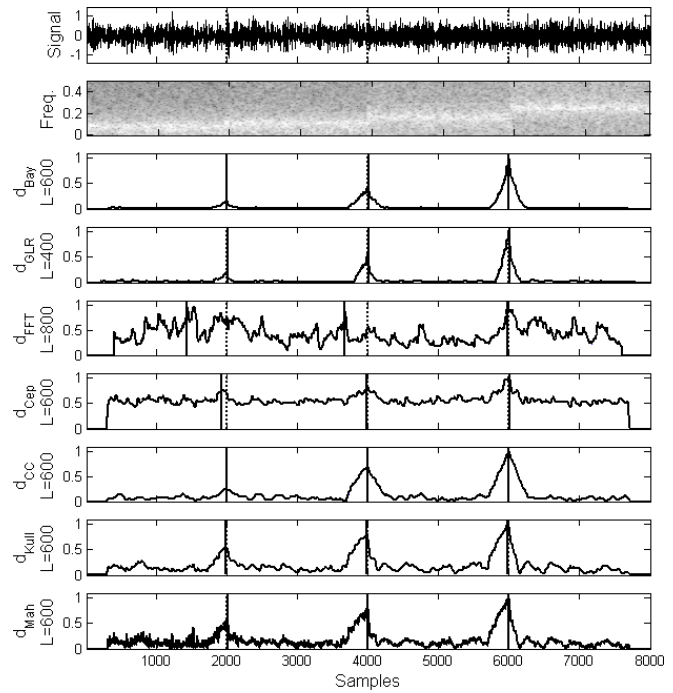


Fig. 3. Curves for all distance measures; dashed lines represent the real position of changes; solid lines represent positions of maxima.

TABLE I  
 MEAN VALUE  $\mu$  AND STANDARD DEVIATION  $\sigma$ . "GOOD" VALUES FOR  $\mu$  ARE DISPLAYED IN BOLD.

change position	"small" 2000	"medium" 4000	"large" 6000
method	$\mu/\sigma$	$\mu/\sigma$	$\mu/\sigma$
$d_{Bay}$	<b>2012/201</b>	<b>4018/200</b>	<b>6006/77</b>
$d_{GLR}$	<b>1994/70</b>	<b>3998/10</b>	<b>5999/6</b>
$d_{FFT}$	2389/1660	<b>3994/1960</b>	5608/1496
$d_{Cep}$	2774/1005	4498/811	6123/354
$d_{CC}$	<b>2003/325</b>	<b>4012/139</b>	<b>5998/8</b>
$d_{Kull}$	2051/393	4053/354	<b>5991/26</b>
$d_{Mah}$	<b>1983/332</b>	<b>4021/227</b>	<b>5994/14</b>

of abrupt changes. The window length  $L$  with the best results has been chosen (the one underlined in the previous list). An example of the curves for the chosen  $L$  with detected maxima is demonstrated in Fig. 3.

Now we will calculate mean value  $\mu$  and standard deviation  $\sigma$  for each position. The mean value should be equal to the real position of the change (2000, 4000, 6000). These statistics are stated in table I, where good results for  $\mu$  (i.e. values that are close to the real position) are displayed in bold.

Let's define set  $\mathcal{M}_\xi$  by the following

$$\mathcal{M}_\xi = \{\hat{m}_i : |\hat{m}_i - m| \leq \xi\}, \quad (3)$$

where  $\hat{m}_i$  stands for the estimated position,  $m$  stands for the real position,  $\xi$  is a tolerance (typically tens of samples). Set  $\mathcal{M}_\xi$  is made up of estimates which are close to the real position. The average "number of hits" (number of cases in which the estimated position is close to the real one) is

$$A_\xi = 100 \cdot \frac{|\mathcal{M}_\xi|}{T_{sig}}, \quad (4)$$

TABLE II  
 AVERAGE "NUMBER OF HITS" IN PERCENT. "GOOD" VALUES ARE  
 DISPLAYED IN BOLD.

change position	"small" 2000	"medium" 4000	"large" 6000
method	$A_{24}/A_{48}$	$A_{24}/A_{48}$	$A_{24}/A_{48}$
$d_{Bay}$	74%/85%	<b>93%/98%</b>	<b>98%/99%</b>
$d_{GLR}$	78%/ <b>92%</b>	<b>95%/100%</b>	<b>99%/100%</b>
$d_{FFT}$	4%/5%	5%/5%	14%/16%
$d_{Cep}$	17%/28%	48%/57%	71%/80%
$d_{CC}$	63%/78%	<b>95%/98%</b>	<b>99%/100%</b>
$d_{Kull}$	62%/78%	80%/ <b>93%</b>	89%/ <b>97%</b>
$d_{Mah}$	61%/74%	88%/ <b>96%</b>	<b>92%/98%</b>

where  $||\mathcal{M}_\xi||$  stands for number of elements in  $\mathcal{M}_\xi$ ,  $T_{sig}$  is the total number of signals; e.g.  $A_{24}$  is the average number of cases in which difference between the estimated and real position is less or equal to 24 samples (3 ms for 8 kHz sampling frequency). Values for  $A_{24}$  and  $A_{48}$  are stated in table II, "good" results (values  $\geq 90\%$ ) are displayed in bold.

We can draw the following conclusions from values in tables I and II:

- The "small" change has been successfully detected only by the GLR distance  $d_{GLR}$  ( $A_{48} = 92\%$ ).
- Best results for the "medium" change have been obtained for the GLR distance  $d_{GLR}$ , the Bayesian detector  $d_{Bay}$  and difference of cepstral coefficients  $d_{CC}$  ( $A_{24} \rightarrow 95\%$ ). But also results for the Kullback divergence and the Mahalanobis distance are not bad ( $A_{48} \rightarrow 95\%$ ).
- The "large" change has been successfully detected by all the detectors except the spectral distance  $d_{FFT}$  and the cepstral distance  $d_{Cep}$ .
- Accuracy of the detection for  $d_{GLR}$ ,  $d_{Bay}$ ,  $d_{CC}$  and  $d_{Mah}$  is outstanding (see values displayed in bold in table I).
- An important quality for most of the detectors is that values of the maxima are increasing together with value of the change (peak in the curve is higher for the "large" change than for the "small" change).

B. Experiment no.2: Pairs of Abrupt Changes With Increasing Distance

Only two filters are used in this experiment. Parameters are following

- filter no. 1:  $r = 0.9$ ,  $\varphi = 40^\circ$ ;
- filter no. 2:  $r = 0.9$ ,  $\varphi = 60^\circ$ .

Positions of changes are 1850, 2000, 3700, 4000, 5550 and 6000; we switch from one filter to other one in each position (see Fig. 4). This setup will lead to a signal, where

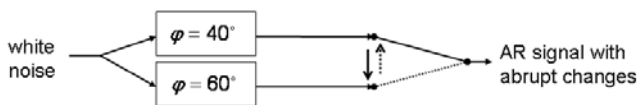


Fig. 4. Structure for generating of AR signal with abrupt changes.

three pairs of changes take place; the distance within the pairs is growing; meaning distance between boundaries of the first

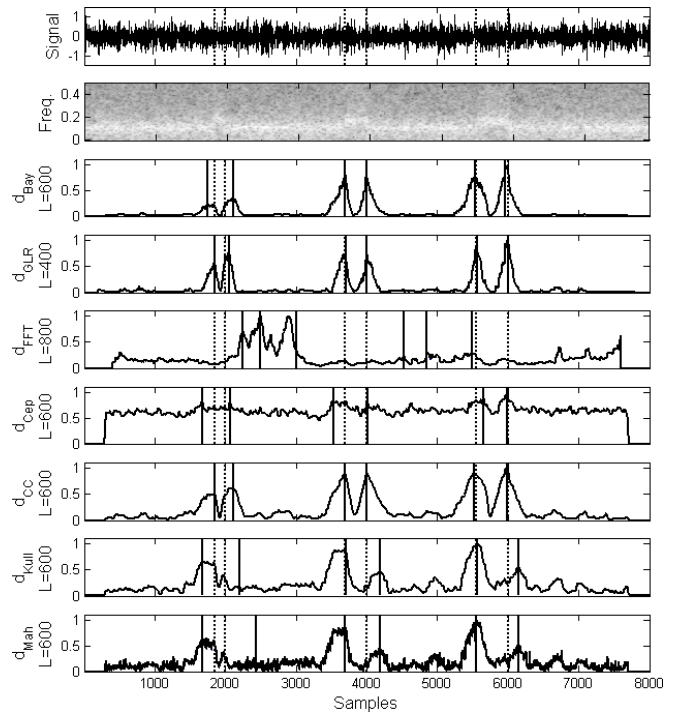


Fig. 5. Curves for all distance measures; dashed lines represent the real position of changes; solid lines represent positions of maxima.

TABLE III  
 AVERAGE "NUMBER OF HITS" IN PERCENT. "GOOD" VALUES ARE  
 DISPLAYED IN BOLD.

change position	"short" 2000	"medium" 4000	"long" 6000
method	$A_{24}/A_{48}$	$A_{24}/A_{48}$	$A_{24}/A_{48}$
$d_{Bay}$	4%/8%	87%/ <b>97%</b>	85%/ <b>98%</b>
$d_{GLR}$	8%/69%	<b>90%/98%</b>	<b>92%/99%</b>
$d_{FFT}$	0%/1%	1%/3%	8%/21%
$d_{Cep}$	2%/6%	54%/74%	49%/73%
$d_{CC}$	5%/65%	89%/ <b>99%</b>	89%/ <b>98%</b>
$d_{Kull}$	4%/6%	26%/32%	26%/36%
$d_{Mah}$	4%/8%	25%/29%	20%/30%

couple is "short" (150 samples), "medium" (300 samples) for the second couple and "long" (450 samples) for the last pair. Note that value of the spectral divergence for each change is approximately the same as for the "medium" change in the experiment no.1. An example of the signal is displayed in Fig. 5.

A total number of 200 signals are generated, each one will be analyzed using the same divergence measures and settings as in the experiment no.1; six maxima are detected in each curve.

The modified "number of hits"  $A_{24}$  and  $A_{48}$  are displayed in table III;  $A_{24}$  is number of cases in which **both** boundaries have been detected correctly (difference between the estimated and real position is  $\leq 24$  samples); definition for  $A_{48}$  is the same.

We can draw the following conclusions from values in table III:

- No method has been able to detect the "short" change

with satisfactory results. Best values were obtained for the GLR distance and difference of cepstral coefficients  $d_{CC}$  ( $A_{48} \rightarrow 65\%$ ).

- The GLR distance  $d_{GLR}$ , the Bayesian detector  $d_{Bay}$  and difference of cepstral coefficients  $d_{CC}$  are able to detect both "medium" and "long" change very precisely ( $A_{48} \rightarrow 98\%$ ).
- The other methods are not able to detect any of the changes. This result is surprising especially for the Kullback divergence  $d_{Kull}$  and the Mahalanobis distance  $d_{Mah}$ ; results for these methods are not bad in experiment no.1. The problem is most likely in detection of the second boundary in the pairs (see the curves in Fig. 5).

### III. CONCLUSION

According to the statistics for both experiments, we can divide the methods into three groups; the GLR distance  $d_{GLR}$ , the Bayesian detector  $d_{Bay}$  and difference of cepstral coefficients  $d_{CC}$  belong into the first one. These methods have outstanding results for the detection of single boundaries (experiment no.1) and very good results for the detection of pairs of boundaries (experiment no.2). Accuracy of detection is excellent for these methods.

The Kullback divergence and the Mahalanobis distance are members of the second group. They are able to detect single boundary very well but results for "couples" are quite bad. Especially detection of the second boundary in the couples is often unsuccessful.

The last group is made up of the cepstral and spectral distance ( $d_{Cep}$  and  $d_{FFT}$ ). Results for both have been unsatisfactory, especially for  $d_{FFT}$ . This poor quality can be a consequence of the fact that these methods do not use the AR model. On the other hand, this might be an advantage for analysis of real signals, which are poorly described by the AR model.

### ACKNOWLEDGMENT

This work has been supported by grants 'Biological and Speech Signal Modeling', GA CR - 102/03/H085; 'Computer analysis of speech and overnight EEG in children', IGA MZ CR - NR 8287-3/2005 and by the research program 'Transdisciplinary Research in Biomedical Engineering 2', MSM6840770012 of the Czech Technical University in Prague.

### REFERENCES

- [1] U. Appel, "A comparative study of three sequential time series segmentation algorithms," *Signal Processing*, vol. 6, pp. 45 – 60, 1984.
- [2] U. Appel, "Adaptive Segmentation of Piecewise Stationary Time Series," *Information Sciences*, no.29, pp. 27 – 56, 1983.
- [3] J.O. Ruanaidh, W.J. Fitzgerald, *Numerical Bayesian Methods Applied to Signal Processing*, Statistics and Computing, Springer, Berlin, 1996.
- [4] R. Cmejla, P. Sovka, "Recursive Bayesian Autoregressive Change-point Detector for Sequential Signal Segmentation," in *EUSIPCO-2004 – Proceedings [CD-ROM]*, Wien: Technische Universität, 2004.
- [5] J.J. Sooful, J.C. Botha, "An acoustic distance measure for automatic cross-language phoneme mapping," *PRASA'01*, pp. 99 – 102, South Africa, November 2001.

- [6] L. Couvreur, J.M. Boite, "Speaker Tracking in Broadcast Audio Material in the Framework of the THISL Project," *Proc. of ESCA ETRW Workshop on Accessing Information in Spoken Audio*, Cambridge (UK), pp. 84 – 89, April 1999.